Association Likelihoods for Directional Estimation

Florian Pfaff, **Kailai Li**, and **Uwe D. Hanebeck**
Intelligent Sensor-Actuator-Systems Laboratory (ISAS)
Institute for Anthropomatics and Robotics
Karlsruhe Institute of Technology (KIT), Germany
florian.pfaff@kit.edu, kailai.li@kit.edu, uwe.hanebeck@kit.edu

***Abstract*—In multitarget tracking, using the association of tracks to measurements that maximizes the association likelihood is a well-established strategy in Euclidean spaces. We explain how this strategy can be adopted for circular domains. Formulae are provided for the association likelihood for three density representations used by important filters for periodic domains—von Mises densities, density approximations based on trigonometric polynomials, and particle-based representations. The presented closed-form formulae allow for efficiently determining the most likely association. In the evaluation, the approaches based on particles and trigonometric polynomials outperform an approach based on a Kalman filter that was adapted to the periodic domain.**

***Index Terms*—Directional statistics, Fourier series, multitarget tracking, particle filter**

I. Introduction

Due to the periodicity of the domain, estimation problems on the unit circle are inherently nonlinear. For periodic domains, filters tailored to the topology at hand can be used to achieve accurate estimation results. In essence, there are three important approaches to topology-aware filtering on periodic manifolds. First, it is possible to use assumed density filters [1], which are similar to filters for linear domains that rely on approximations involving densities of a certain class, such as Gaussian densities. Second, particle filters [2], which constitute a very general nonlinear estimation approach, can be used. On periodic domains, the particles can be propagated through a topology-aware function and then reweighted and redrawn as in a standard particle filter approach. Third, there are approaches that use the finite size of the domain to their advantage [3], [4]. Examples of such filters are the Fourier filters [3], in which the density or its square root is approximated using a trigonometric polynomial (i.e., a Fourier series with a finite number of nonzero coefficients).

So far, estimators for periodic manifolds only allowed for tracking single targets. However, a variety of real-world scenarios exist in which it is necessary to track multiple targets that cannot be distinguished simultaneously. Such applications include tracking space debris, which can be modeled to be located on a spherical manifold [5]. Further, scenarios exist in which it is possible to measure the orientation of multiple objects but no information is available regarding which measurement stems from which object [6]. While significant research has gone into multitarget tracking for linear domains [7], [8], little research has been conducted on multitarget tracking for periodic domains.

In this paper, we limit ourselves to approaches that perform one-to-one assignments. In such approaches, a so-called hard (or explicit) association decision is used to assign each measurement to (at most) a single track. A popular aim is to find the most likely association, maximizing the so-called global association likelihood [8, Sec. 10.3.1.4]. A closely related concept is the global nearest neighbor (GNN) [7, Sec. 6.4], [8, Sec. 10.3.1.3], in which the sum of squared (uncertainty-aware) Mahalanobis distances is minimized. Based on the squared Mahalanobis distances of all measurement–track pairs, the association decision can be obtained by solving a linear assignment problem. For Gaussian densities, the association obtained via the GNN can be shown to yield the highest association likelihood. For more details on the relationship between the maximization of the association likelihood and the GNN, we refer the reader to [9, Sec. 11.3].

In early approaches to multitarget tracking, only information about each target's motion in linear (Euclidean) spaces was considered for deriving the associations. Integrating additional features into the association process was proposed, e.g., in [10], [11]. In these works, it is proposed to treat features on non-periodic continuous domains like the positions of the targets in a classical multitarget tracking approach. Further, the papers address features that can attain a number of discrete values or should fall into a set of known categories. For features on continuous domains, it is implied that modifications may be required if the densities are clearly non-Gaussian.

Recently, we presented an efficient approach to integrate periodic quantities into a multitarget tracking algorithm without assuming the densities to be Gaussian distributed [6]. The extended algorithm, which can handle both linear and periodic quantities, was applied to tracking for optical belt sorting. For some tracking tasks in this context, measurements of both the position and orientation of the targets are available. Squared Mahalanobis distances were calculated for the position part, which was modeled to be perturbed by Gaussian-distributed noise. For the periodic part of the state, a distance measure on the circle was employed. A weighted combination of these two distances was calculated in each time step for deciding on an association. The approach employed in [6] helped to improve the tracking results compared with an algorithm that

does not respect the orientation in the association. However, the association used was generally not the most probable for the system and measurement model employed. In our current paper, we focus on state spaces with the topology of the unit circle, which we parameterize by $[0, 2\pi)$, and explicate how the most probable association decision can be derived.

The paper is structured as follows. In Sec. II, we describe the density representations used by important filters for circular manifolds. In Sec. III, we derive closed-form formulae for the association likelihood for the individual representations. How the most likely association can be derived based on these formulae is explained in the fourth section. Evaluations are given for the individual approaches in Sec. V, and a conclusion and an outlook are provided in Sec. VI.

II. Density Representations Used by Filters for Circular Manifolds

One notable filter for circular manifolds is the von Mises filter [1]. It is based on the assumption that the prior and posterior densities can be approximated well using von Mises densities. The density of a von Mises distribution comprises an exponential function and a normalization constant. The formula

$$f_{\mathrm{VM}}(x; \mu, \kappa) = \frac{1}{2\pi I_0(\kappa)} \mathrm{e}^{\kappa \cos(x-\mu)}$$

involves a location parameter μ, a concentration parameter κ, and the Bessel function of the first kind of order zero $I_0(\cdot)$. When two von Mises densities are multiplied and the result is normalized, a von Mises density is obtained [1]. Thus, for von Mises-distributed prior densities and likelihoods, a precise update step can be realized. However, this does not hold for the prediction step. Even if a simple system model is employed and all noise terms are von Mises distributed, the prediction result is generally not von Mises distributed. Thus, approximations are generally inevitable in the von Mises filter.

In the particle filter, the prior and posterior densities are represented using a finite number of (potentially weighted) samples. The samples and their weights can be interpreted to describe a mixture of Dirac delta distributions, which is also referred to as wrapped Dirac mixture [12] on the circle. Such a mixture can be written as

$$f_{\mathrm{WD}}(x; \underline{s}, \underline{w}) = \sum_{k=1}^{L} w_k \delta(x - s_k) \ ,$$

depending on the vector of positions $\underline{s}$ and vector of weights $\underline{w}$ for the L samples. All weights should be nonnegative and sum up to one. Such a representation is also used by a Dirac-based discrete filter [4], in which the positions of the individual components are static.

Last, we address the representations used by the Fourier filters. In the Fourier identity filter, each density is represented by a vector of Fourier coefficients $\underline{c} = [c_{-k_{\max}}, \ldots, c_{k_{\max}}]^\top$ comprising $2k_{\max} + 1$ entries according to

$$f(x; \underline{c}) = \sum_{k=-k_{\max}}^{k_{\max}} c_k \mathrm{e}^{\mathrm{i}kx} \ ,$$

with i denoting the imaginary unit. The density can always be ensured to integrate to 1. However, ensuring that the approximations of all functions involved have no negative values is nontrivial. Further, the nonnegativity is generally not preserved throughout update steps when truncation is used to prevent an increase in the number of parameters.

As an alternative that ensures the nonnegativity of the approximation, the Fourier square root filter was proposed. The Fourier square root filter is based on approximating the square root of the density using a trigonometric polynomial with coefficient vector[1] $\underline{d} = [d_{-k_{\max}}, \ldots, d_{k_{\max}}]^\top$. The density is then approximated by

$$f(x; \underline{d}) = \left(\sum_{k=-k_{\max}}^{k_{\max}} d_k \mathrm{e}^{\mathrm{i}kx} \right)^2 \ .$$

In this representation, both the normalization and the nonnegativity of the density can be preserved throughout prediction and update steps without an increase in the number of parameters.

III. Derivation of the Association Likelihoods

In this section, we begin by providing and reformulating a general expression for the association likelihood. We say there are n tracks and m measurements and index them by $i \in \{1, \ldots, n\}$ and $j \in \{1, \ldots, m\}$. The state of the ith track is denoted by x^i and the jth measurement by $\hat{z}^j$. The association likelihood $\ell(\hat{z}^j|i)$ can be obtained by considering the joint likelihood $\ell(\hat{z}^j, x^i|i)$ and marginalizing out x^i, i.e.,

$$\ell(\hat{z}^j|i) = \int_{\Omega_{\boldsymbol{x}}} \ell(\hat{z}^j, x^i|i) \, dx^i \ ,$$

in which $\Omega_{\boldsymbol{x}}$ denotes the sample space of the track's state, which is $[0, 2\pi)$ for circular domains. A reformulation yields

$$\ell(\hat{z}^j|i) = \int_{\Omega_{\boldsymbol{x}}} \ell(\hat{z}^j|x^i, i) f(x^i|i) \, dx^i \ .$$

As $\hat{z}^j$ is conditionally independent of i given x^i, $\ell(\hat{z}^j|x^i, i)$ can be replaced by the measurement likelihood $f^{\mathrm{L},j}(\hat{z}^j|x^i)$. The density describing the state of the track i (based on the initial prior density and all measurements assigned to the track so far) is given by the prior density $f^{\mathrm{p},i}(x^i)$. Thus, we obtain

$$\ell(\hat{z}^j|i) = \int_{\Omega_{\boldsymbol{x}}} \underbrace{f^{\mathrm{L},j}(\hat{z}^j|x^i) f^{\mathrm{p},i}(x^i)}_{\check{f}^{\mathrm{e},i,j}(x^i)} \, dx^i \ . \tag{1}$$

For Gaussian densities, a closed-form expression for the association likelihood is well known (see [8, Section 10.3, Equations (10.22)–(10.26)]). In the subsections of this section, we provide closed-form formulae for the association likelihood for the representations of periodic densities described in Sec. II. We start by deriving the association likelihood for von Mises densities, then address wrapped Dirac mixtures, and finally provide formulae for the representations based on trigonometric polynomials.

[1] In our other works, e.g., [3], [13], we use $\underline{c}^{\mathrm{id}}$ instead of $\underline{c}$ and $\underline{c}^{\mathrm{sqrt}}$ instead of $\underline{d}$. For our current contribution, keeping the number of upper indices to a minimum allows for a clearer notation.

Remark 1. For updating the ith track with the jth measurement, Bayes' formula yields

$$f^{\mathrm{e},i,j}(x^i) = \frac{f^{\mathrm{L},j}(\hat{z}^j|x^i) f^{\mathrm{p},i}(x^i)}{\int_{\Omega_{\boldsymbol{x}}} f^{\mathrm{L},j}(\hat{z}^j|x^i) f^{\mathrm{p},i}(x^i)\,dx^i} = \frac{\breve{f}^{\mathrm{e},i,j}(x^i)}{\int_{\Omega_{\boldsymbol{x}}} \breve{f}^{\mathrm{e},i,j}(x^i)\,dx^i}$$

for the posterior density $f^{\mathrm{e},i,j}(x^i)$. Since the formula in the denominator is equivalent to the formula for the association likelihood (1), the association likelihood is the reciprocal of the normalization constant in the Bayes' formula. Further, the association likelihood is the reciprocal of the integral over the unnormalized posterior density obtained by multiplying the prior density with the likelihood. In Fig. 1, we consider an example involving one track and multiple measurements. We illustrate the prior densities, likelihoods, posterior densities, and association likelihoods for the von Mises filter, particle filter, and Fourier square root filter.

A. Von Mises Filter

In our derivation of the association likelihood, we proceed similarly as in [13, App. E]. First, we write out (1) for von Mises densities. The prior density of the ith track is given by $f_{\mathrm{VM}}(x^i; \hat{x}^{\mathrm{p},i}, \kappa^{\mathrm{p},i})$, and the measurements are generated according to a topology-aware identity model with additive von Mises-distributed noise, resulting in a likelihood of $f_{\mathrm{VM}}(\hat{z}^j; x^i, \kappa^{\boldsymbol{v},j})$. Thus, we obtain

$$\begin{aligned}\ell(\hat{z}^j|i) &= \int_0^{2\pi} f_{\mathrm{VM}}(\hat{z}^j; x^i, \kappa^{\boldsymbol{v},j}) f_{\mathrm{VM}}(x^i; \hat{x}^{\mathrm{p},i}, \kappa^{\mathrm{p},i})\,dx^i \\ &= \int_0^{2\pi} \frac{1}{2\pi I_0(\kappa^{\boldsymbol{v},j}) 2\pi I_0(\kappa^{\mathrm{p},i})} \\ &\qquad \cdot \mathrm{e}^{\kappa^{\boldsymbol{v},j}\cos(\hat{z}^j - x^i)} \mathrm{e}^{\kappa^{\mathrm{p},i}\cos(x^i - \hat{x}^{\mathrm{p},i})} dx^i\ . \end{aligned} \tag{2}$$

The expression in the integral is a multiplication of the two von Mises densities $f_{\mathrm{VM}}(x^i; \hat{x}^{\mathrm{p},i}, \kappa^{\mathrm{p},i})$ and $f_{\mathrm{VM}}(\hat{z}^j; x^i, \kappa^{\boldsymbol{v},j}) = f_{\mathrm{VM}}(x^i; \hat{z}^j, \kappa^{\boldsymbol{v},j})$. From the formula for the update step of the von Mises filter [1], we know that the multiplication result is proportional to a von Mises density with the parameters

$$C = \kappa^{\mathrm{p},i}\cos(\hat{x}^{\mathrm{p},i}) + \kappa^{\boldsymbol{v},j}\cos(\hat{z}^j)\ , \tag{3}$$

$$S = \kappa^{\mathrm{p},i}\sin(\hat{x}^{\mathrm{p},i}) + \kappa^{\boldsymbol{v},j}\sin(\hat{z}^j)\ , \tag{4}$$

$$\hat{x}^{\mathrm{e},i,j} = \operatorname{atan2}(S, C)\ , \tag{5}$$

$$\kappa^{\mathrm{e},i,j} = \sqrt{C^2 + S^2}\ . \tag{6}$$

Hence, we obtain

$$\begin{aligned}&\frac{1}{2\pi I_0(\kappa^{\boldsymbol{v},j}) 2\pi I_0(\kappa^{\mathrm{p},i})} \mathrm{e}^{\kappa^{\boldsymbol{v},j}\cos(\hat{z}^j - x^i)} \mathrm{e}^{\kappa^{\mathrm{p},i}\cos(x^i - \hat{x}^{\mathrm{p},i})} \\ &\qquad \propto \frac{1}{2\pi I_0(\kappa^{\mathrm{e},i,j})} \mathrm{e}^{\kappa^{\mathrm{e},i,j}\cos(x^i - \hat{x}^{\mathrm{e},i,j})}\end{aligned}$$

and thus also

$$\mathrm{e}^{\kappa^{\boldsymbol{v},j}\cos(\hat{z}^j - x^i)} \mathrm{e}^{\kappa^{\mathrm{p},i}\cos(x^i - \hat{x}^{\mathrm{p},i})} \propto \mathrm{e}^{\kappa^{\mathrm{e},i,j}\cos(x^i - \hat{x}^{\mathrm{e},i,j})}\ . \tag{7}$$

In App. A, we show that (7) is actually an equality. This allows us to rewrite (2) as

$$\ell(\hat{z}^j|i) = \frac{1}{2\pi I_0(\kappa^{\boldsymbol{v},j}) 2\pi I_0(\kappa^{\mathrm{p},i})} \int_0^{2\pi} \mathrm{e}^{\kappa^{\mathrm{e},i,j}\cos(x^i - \hat{x}^{\mathrm{e},i,j})} dx^i\ .$$

The integral over the exponential function is the reciprocal of the normalization constant of the von Mises density with circular mean $\hat{x}^{\mathrm{e},i,j}$ and concentration parameter $\kappa^{\mathrm{e},i,j}$. Using the formula for the normalization constant, we obtain the formula

$$\ell(\hat{z}^j|i) = \frac{I_0(\kappa^{\mathrm{e},i,j})}{2\pi I_0(\kappa^{\boldsymbol{v},j}) I_0(\kappa^{\mathrm{p},i})}$$

for the association likelihood.

B. Particle Filter

As explained in Sec. II, the particle filter can be interpreted to use a wrapped Dirac mixture to represent the prior density. To perform an update step, we require a likelihood function that can be evaluated for arbitrary values $x \in [0, 2\pi)$. Given such a likelihood function, we obtain

$$\begin{aligned}\ell(\hat{z}^j|i) &= \int_{[0,2\pi)} f^{\mathrm{L},j}(\hat{z}^j|x^i) f^{\mathrm{p},i}(x^i)\,dx^i \\ &= \int_{[0,2\pi)} f^{\mathrm{L},j}(\hat{z}^j|x^i) \sum_{k=1}^{L} w_k^i \delta(x^i - s_k^i)\,dx^i\end{aligned} \tag{8}$$

as the formula for the association likelihood. We specifically use the half-open interval to avoid any confusion as to how the first integral is defined if there is a sample at $x^i = 0$. Using the properties of the Dirac delta distribution, the closed-form expression

$$\ell(\hat{z}^j|i) = \sum_{k=1}^{L} w_k^i f^{\mathrm{L},j}(\hat{z}^j|s_k^i) \tag{9}$$

can be derived from (8). This formula can also be used for the discrete filter presented in [4] that uses the same representation of the prior density.

C. Fourier Filters

To derive the formulae for the association likelihood for the Fourier filters, we proceed similarly as in [13, Sec. 7.1.2]. We begin by considering the Fourier identity filter. As the first step to obtaining a closed-form expression for (1), we calculate the Fourier coefficients of $\breve{f}^{\mathrm{e},i,j}$. The Fourier coefficient vector of the multiplication of two functions represented by their Fourier coefficient vectors is equal to the discrete convolution (denoted by $*$) of the two coefficient vectors. Thus, if $\underline{c}^{\mathrm{L},j}$ is the Fourier coefficient vector of $f^{\mathrm{L},j}$ and $\underline{c}^{\mathrm{p},i}$ is the Fourier coefficient vector of $f^{\mathrm{p},i}$, the Fourier coefficient vector $\breve{\underline{c}}^{\mathrm{e},i,j}$ representing the unnormalized posterior density $\breve{f}^{\mathrm{e},i,j}$ can be calculated according to

$$\breve{\underline{c}}^{\mathrm{e},i,j} = \underline{c}^{\mathrm{L},j} * \underline{c}^{\mathrm{p},i}\ .$$

The integral of a Fourier series over $[0, 2\pi)$ is equal to the zeroth coefficient multiplied by 2π [13, Sec. 6.2.2]. Using the formula for the convolution, we obtain

$$\ell(\hat{z}^j|i) = 2\pi \breve{c}_0^{\mathrm{e},i,j} = 2\pi \sum_{k=-k_{\max}}^{k_{\max}} c_k^{\mathrm{L},j}\, c_{-k}^{\mathrm{p},i}\ . \tag{10}$$

This formula can also be expressed as a vector–vector multiplication. For real functions, the Fourier coefficient with index

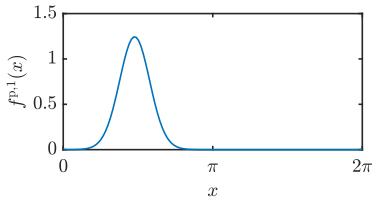

(a) True von Mises prior density as used by the von Mises filter.

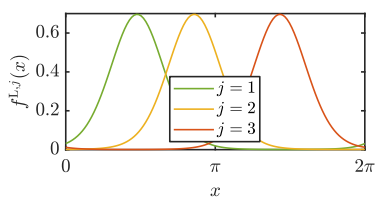

(b) Von Mises approximations of the likelihoods.

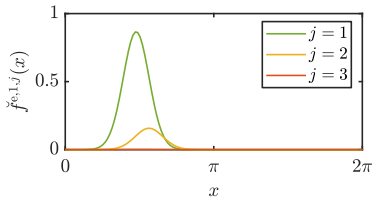

(c) Unnormalized posterior densities obtained by multiplying the von Mises approximations of the likelihoods with the prior density.

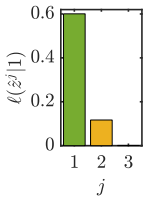

(d) Association likelihoods (von Mises filter).

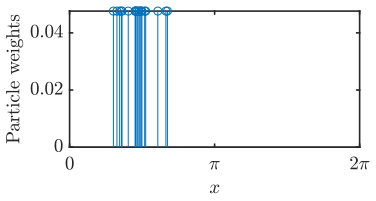

(e) A possible representation of the prior density used by the particle filter (obtained via random sampling).

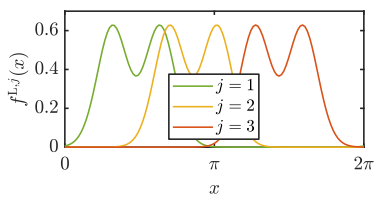

(f) True likelihoods used by the particle filter.

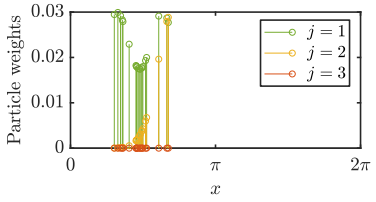

(g) Weighted samples representing the posterior densities (result of the particle filter before resampling is employed).

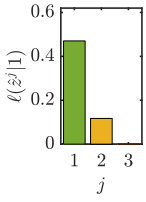

(h) Association likelihoods (particle filter).

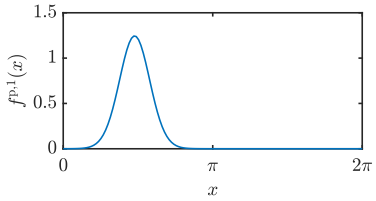

(i) Approximation of the prior density used by the Fourier square root filter.

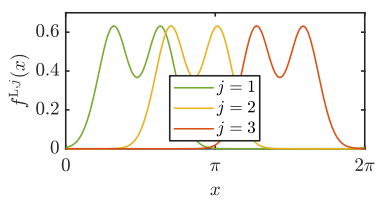

(j) Trigonometric polynomial-based approximations of the likelihoods.

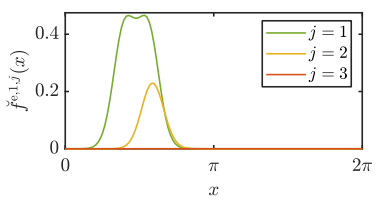

(k) Posterior densities before the normalization obtained by using the Fourier square root filter.

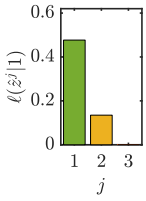

(l) Association likelihoods (Fourier filter).

Figure 1. The compatibility of one track to three measurements is assessed by using the von Mises filter, the particle filter, and the Fourier square root filter. For the Fourier filter, 21 coefficients are used and 21 particles are used for the particle filter. The true prior density is a von Mises density and von Mises mixtures are used as the likelihoods. For each filter, the representations of the prior density and the likelihoods are given. Moreover, the corresponding unnormalized posterior densities are depicted along with the resulting association likelihoods. We do not depict the ground truth results as a reference because the results are visually indistinguishable from those of the Fourier square root filter. As we only consider a single track, we omit the upper index of x that is used in the formulae for the derivation of the association likelihoods.

$-k$ is the complex conjugate of the Fourier coefficient with index k. Thus, we obtain

$$\ell(\hat{z}^j|i) = 2\pi\,(\underline{c}^{\mathrm{L},j})^\top \overline{\underline{c}}^{\mathrm{p},i}\ . \tag{11}$$

By concatenating the vectors $(\underline{c}^{\mathrm{L},j})^\top$ vertically and $\overline{\underline{c}}^{\mathrm{p},i}$ horizontally for all indices, two matrices are obtained, which, when multiplied, yield a matrix containing the coefficients $\breve{c}_0^{\mathrm{e},i,j}$ for all combinations of tracks and measurements.

As mentioned in Sec. II, the approximations of the functions used in the Fourier identity filter may have negative function values. If the likelihood or the prior density have negative function values, the association likelihood may be negative, which is not a valid value for a likelihood. If (11) yields a negative value when a valid association likelihood is required, it can make sense to replace the value with its absolute value or zero.

For the Fourier square root filter, there are two ways to obtain the association likelihood. The first involves determining the coefficient vectors $\underline{c}^{\mathrm{L},j}$ and $\underline{c}^{\mathrm{p},j}$ directly describing the prior density and likelihood from the coefficient vectors $\underline{d}^{\mathrm{L},j}$ and $\underline{d}^{\mathrm{p},j}$ describing their square roots using

$$\underline{c}^{\mathrm{L},j} = \underline{d}^{\mathrm{L},j} * \underline{d}^{\mathrm{L},j}\ , \qquad \underline{c}^{\mathrm{p},j} = \underline{d}^{\mathrm{p},j} * \underline{d}^{\mathrm{p},j}\ .$$

Then, the same formula as for the Fourier identity filter can be employed. Since the functions represented by $\underline{c}^{\mathrm{L},j}$ and $\underline{c}^{\mathrm{p},i}$ are nonnegative everywhere, the multiplication result represented by $\breve{\underline{c}}^{\mathrm{e},i,j}$ is also nonnegative. Further, since the trigonometric polynomials approximating the prior density and likelihood can only have a finite number of roots, the integral over $\breve{f}^{\mathrm{e},i,j}$ is always positive for the Fourier square root filter.

In the second way to obtain the association likelihood, we begin by calculating the coefficient vector $\breve{\underline{d}}^{\mathrm{e},i,j}$ representing the square root of the unnormalized posterior density via

$$\breve{\underline{d}}^{\mathrm{e},i,j} = \underline{d}^{\mathrm{L},j} * \underline{d}^{\mathrm{p},i}\ .$$

Then, we can use Parseval's formula [14, Vol. I, Sec. II.1, Thm. 1.12] to obtain a formula for the integral over the square

of the function. Thus, we obtain the formula

$$\ell(\hat{z}^j|i) = 2\pi\left\|\underline{d}^{\mathrm{e},i,j}\right\|^2 = 2\pi\left\|\underline{d}^{\mathrm{L},j} * \underline{d}^{\mathrm{p},i}\right\|^2$$

for all combinations of indices i and j.

IV. Determining the Most Likely Association

For simplicity, we limit ourselves to equal numbers of tracks and measurements, i.e., $n = m$. In this case, an association can be described by a permutation τ mapping each track index to a measurement index. The most likely permutation maximizes

$$\ell(\hat{z}^{\tau(1)}, \hat{z}^{\tau(2)}, \ldots, \hat{z}^{\tau(n)}|1, 2, \ldots, n) = \prod_{i=1}^{n} \ell(\hat{z}^{\tau(i)}|i) \ . \quad (12)$$

The same permutation minimizes

$$-\log \ell(\hat{z}^{\tau(1)}, \hat{z}^{\tau(2)}, \ldots, \hat{z}^{\tau(n)}|1, 2, \ldots, n) = -\sum_{i=1}^{n} \log \ell(\hat{z}^{\tau(i)}|i),$$

which is the negative logarithm of (12). This formula motivates the so-called association matrix [9, Ch. 11] containing the negative logarithms of the association likelihoods for all combinations of indices i and j. Based on this matrix, the permutation resulting in the smallest sum can be obtained via a solver for linear assignment problems (LAPs), such as the LAPJV [15].

If a closed-form formula for the association likelihood is known, the logarithms of the association likelihoods can be calculated efficiently. However, the actual negative logarithms of the association likelihoods may not be required to obtain the optimal association. In some cases, it is possible to simplify the formula for the entries of the matrix by performing changes that do not alter the optimal permutation derived. Such a simplified formula is derived for multivariate Gaussian densities in [8, Section 10.3, Equations (10.27)–(10.29)].

For the von Mises filter, the negative sum of the logarithms can be reformulated according to

$$\begin{aligned}
&-\sum_{i=1}^{n} \log\left(\frac{I_0(\kappa^{\mathrm{e},i,\tau(i)})}{2\pi I_0(\kappa^{\boldsymbol{v},\tau(i)}) I_0(\kappa^{\mathrm{p},i})}\right) \\
&= \sum_{i=1}^{n} -\log\left(I_0(\kappa^{\mathrm{e},i,\tau(i)})\right) \\
&\quad + n2\pi + \sum_{i=1}^{n} \log\left(I_0(\kappa^{\boldsymbol{v},\tau(i)})\right) + \sum_{i=1}^{n} \log\left(I_0(\kappa^{\mathrm{p},i})\right) \\
&= \sum_{i=1}^{n} -\log\left(I_0(\kappa^{\mathrm{e},i,\tau(i)})\right) \\
&\quad \underbrace{+ n2\pi + \sum_{i=1}^{n} \log\left(I_0(\kappa^{\boldsymbol{v},i})\right) + \sum_{i=1}^{n} \log\left(I_0(\kappa^{\mathrm{p},i})\right)}_{\text{independent of } \tau} \ .
\end{aligned}$$

All additive terms that are independent of the permutation τ can be disregarded because they do not influence which permutation minimizes the expression. By applying an LAP solver to the matrix containing the entries $-\log\left(I_0(\kappa^{\mathrm{e},i,j})\right)$ for all i and j, the most likely association can be derived.

For the particle filter, the entries of the association matrix can be determined by calculating the negative logarithm of the association likelihood obtained via (9). For the Fourier filters, we have to be aware that (10) can result in negative values for the Fourier identity filter. If an association likelihood of zero or less is obtained, a large value can be used as the entry of the association matrix. This makes it (almost) impossible that the respective track–measurement pair is part of the association obtained using the LAP solver.

For filters for which no closed-form formula for the association likelihood is known, a way to efficiently generate suboptimal values for the association matrix can be used instead. Using a measure of distance between the circular means of the likelihood and the prior density as a substitute for the actual negative logarithm of the likelihood can lead to good association results. In [6], the cosine distance

$$d_{\cos}(\hat{x}^{\mathrm{p},i}, \hat{z}^j) = 1 - \cos(\hat{x}^{\mathrm{p},i} - \hat{z}^j)$$

was used as the distance measure. A downside of this approach is that the uncertainties are not taken into account. Further, the circular means need to be well defined, which may not be the case, e.g., for antipodally symmetric densities. In such cases, reformulating the estimation problem may make it possible to use the distance-based association process nonetheless [6].

V. Evaluation

In our evaluation, we compare five different filters. The first four filters are the filters for which the association likelihoods were presented in this paper, namely the von Mises filter, the particle filter, the Fourier identity filter, and the Fourier square root filter. For all of these filters, the association matrices are generated as explained in Sec. IV. For the particle filter and the Fourier filters, different numbers of parameters are employed. As the fifth filter, an adapted version of the Kalman filter is considered. The adapted Kalman filter can be interpreted as follows. If the means of the prior density and the likelihood are more than π apart, the border of periodicity is shifted so that the means are no longer more than π apart. This significantly improves the estimation quality as the periodicity of the estimation problem is taken into account to some degree. For the Kalman filter-based multitarget tracking, the entries of the association matrix are calculated according to the cosine distance. Experiments with an adapted version of the Mahalanobis distance showed that using the cosine distance yields better results, which is why only the results based on the cosine distance are provided in our evaluation.

The filters are compared based on the number of association errors. In Fig. 2, we illustrate how the errors are counted. The initial assignment of measurements to tracks is irrelevant to our error measure. In every further step, if the measurement associated with a track does not stem from the same object as the measurement that was associated with the track in the previous time step, this is counted as an error. In our scenarios, we have a constant number of tracks, and thus, a single error cannot occur in isolation. As illustrated in Fig. 2, confusing two objects is counted as two errors. When the association is

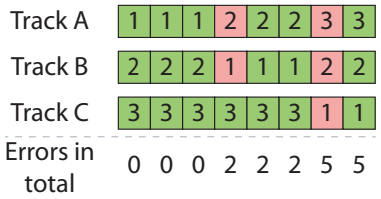

Figure 2. Illustration of how the association errors are counted. The number in each box is the ID of the actual object from which the measurement stems.

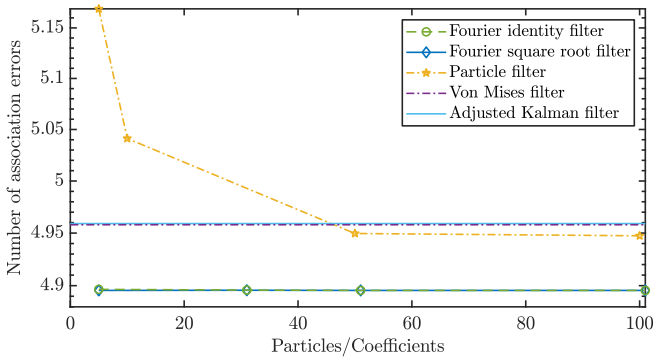

Figure 3. Number of association errors for the individual filters in the scenario involving only von Mises-distributed noise terms. The results of the von Mises filter and the Kalman filter are given as horizontal lines because the number of parameters cannot be varied. These two lines are almost identical due to the very similar performance of the filters. The same holds for the lines of the two Fourier filters.

incorrect for more than two tracks in one time step, the number of errors corresponds to the number of tracks for which the new measurement stems from a different object than in the previous time step.

We consider a simulated tracking scenario involving multiple objects that move along a circular path at an approximately constant, known velocity. This can, for example, be seen as a simplified version of a task to track objects in an identical orbit in space. Five objects are tracked for nine time steps. The concentration parameter of all prior densities is $\kappa = 10$ and the individual means are placed at every integer from 1 to 5. Thus, the distance between neighboring objects is 1, except for the distance between the last and the first object. The true initial values are drawn from the individual prior densities.

A topology-aware identity model with additive noise is used as the system and measurement model. This means, for every time step t and object i, the random variable (written in bold letters) for the measurement $\boldsymbol{z}_t^{\tau(i)}$ is a topology-aware sum of the respective state $\boldsymbol{x}_t^i$ and the measurement noise $\boldsymbol{v}_t^{\tau(i)}$, i.e.,

$$\boldsymbol{z}_t^{\tau(i)} = \boldsymbol{x}_t^i + \boldsymbol{v}_t^{\tau(i)} \mod 2\pi \ .$$

Further, the state of the object i at the next time step $t+1$ is given by

$$\boldsymbol{x}_{t+1}^i = \boldsymbol{x}_t^i + \boldsymbol{u}_t^i \mod 2\pi \ , \qquad \boldsymbol{u}_t^i = c + \boldsymbol{w}_t^i \ ,$$

with a constant c describing the displacement in every time step caused by the constant velocities of the objects. As the

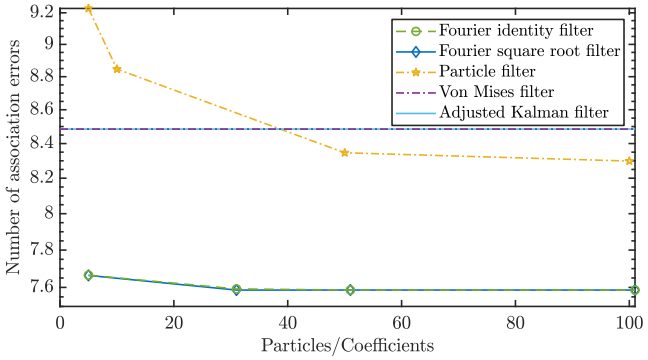

Figure 4. Number of association errors in the scenario involving a von Mises mixture as the measurement noise. Again, the lines for the Kalman filter and the von Mises filter are identical, which holds similarly for the lines of the Fourier filters.

means of the velocities of all objects are identical and known, the estimation problem can be reduced to one involving objects that perform a topology-aware random walk according to the system noise $\boldsymbol{w}_t^i$. The noise terms $\boldsymbol{v}_t^{\tau(i)}$ and $\boldsymbol{w}_t^i$ are distributed according to a von Mises distribution with $\mu = 0$ and $\kappa = 30$ in every time step.

The scenario was simulated 20000 times and the associations were recorded for all approaches. The maximum number of association errors is equal to the number of time steps minus one multiplied by the number of objects, which yields 40 in the described scenario. A certain number of association errors may be inevitable for the system model used. When one object passes another, even a perfect filter based on noise-free measurements may deem an incorrect association to be the most likely.

The evaluation results are shown in Fig. 3. The two Fourier filters perform equally well and outperform all other filters evaluated. The association quality of the particle filter surpasses those of the adapted Kalman filter and the von Mises filter but does not reach the quality of the Fourier filters even for high numbers of samples. The number of association errors of the von Mises filter is only slightly different from the number achieved using the adapted Kalman filter. This indicates that calculating the cosine distance is a viable alternative to determining the actual negative logarithm of the association likelihood.

To provide a more comprehensive evaluation, we also consider a modified version of the scenario, in which the measurement noise density is a mixture of von Mises densities according to

$$\boldsymbol{v}_t^{\tau(i)} \sim \frac{1}{2} f_{\mathrm{VM}}(v_t^{\tau(i)}; 2\pi - 0.3, 50) + \frac{1}{2} f_{\mathrm{VM}}(v_t^{\tau(i)}; 0.3, 50) \ .$$

Further, the system noise density was replaced by a von Mises density with $\kappa = 50$. While the numbers of errors shown in Fig. 4 are different from those in the original scenario, the results clearly resemble. A notable difference is that the absolute differences in the qualities of the filters are higher in

the modified scenario. Further, the Fourier filters require more coefficients to achieve their optimal performance.

VI. Conclusion

In this paper, we have presented formulae for the association likelihood for density representations used by important filters for circular domains. The formulae allow for efficiently determining the most likely association for multitarget tracking when one of the considered filters is used. Since all formulae presented are in closed form, they can be used even in real-time applications. In the evaluation, we showed that the multitarget tracking approaches based on the particle filter and the Fourier filters outperform a Kalman filter-based approach. The von Mises filter-based multitarget tracking, however, did not prove to be superior to the Kalman filter-based tracking. Future work includes considering density representations on higher dimensional manifolds such as the torus or the unit sphere.

Appendix

To prove that (7) is an equality, we first drop the indices i and j to obtain more compact expressions. Since the left-hand and right-hand sides of (7) are proportional and nonzero for all input values, it is sufficient to show that the equality holds for a single input value x. We choose $x = 0$ and prove

$$\mathrm{e}^{\kappa^{\boldsymbol{v}} \cos(\hat{z})} \mathrm{e}^{\kappa^{\mathrm{p}} \cos(\hat{x}^{\mathrm{p}})} = \mathrm{e}^{\kappa^{\mathrm{e}} \cos(\hat{x}^{\mathrm{e}})} \ . \tag{13}$$

The left-hand side of (13) can be rewritten using a single exponent. Further, due to the strict monotonicity of the exponential function, it is sufficient to show

$$\kappa^{\boldsymbol{v}} \cos(\hat{z}) + \kappa^{\mathrm{p}} \cos(\hat{x}^{\mathrm{p}}) = \kappa^{\mathrm{e}} \cos(\hat{x}^{\mathrm{e}}) \tag{14}$$

to prove (13).

We now write out $\hat{x}^{\mathrm{e}}$ to obtain

$$\cos(\hat{x}^{\mathrm{e}}) = \cos(\operatorname{atan2}(S, C)) \ .$$

Next, we use $\cos(\operatorname{atan}(\alpha)) = \frac{1}{\sqrt{1+\alpha^2}}$ [16] and consider the $\operatorname{atan2}$ for all quadrants and quadrant borders [17] separately, yielding

$$\cos(\hat{x}^{\mathrm{e}}) = \begin{cases} \cos(\operatorname{atan}(S/C)) & \\ \quad = \frac{1}{\sqrt{1+S^2/C^2}} = \frac{C}{\sqrt{C^2+S^2}} & C > 0,\ S > 0 \\ \cos(\pi + \operatorname{atan}(S/C)) & \\ \quad = -\frac{1}{\sqrt{1+S^2/C^2}} = -\frac{|C|}{\sqrt{C^2+S^2}} & C < 0,\ S > 0 \\ \quad = \frac{C}{\sqrt{C^2+S^2}} & \\ \cos(-\pi + \operatorname{atan}(S/C)) & \\ \quad = \cos(\pi + \operatorname{atan}(S/C)) & C < 0,\ S < 0 \\ \quad = \frac{C}{\sqrt{C^2+S^2}} & \\ \cos(\operatorname{atan}(S/C)) = \frac{C}{\sqrt{C^2+S^2}} & C > 0,\ S < 0 \\ \cos(0) = 1 = \frac{C}{\sqrt{C^2}} = \frac{C}{\sqrt{C^2+S^2}} & C > 0,\ S = 0 \\ \cos\left(\frac{\pi}{2}\right) = 0 = \frac{C}{\sqrt{C^2+S^2}} & C = 0,\ S > 0 \\ \cos(\pi) = -1 = \frac{C}{\sqrt{C^2}} = \frac{C}{\sqrt{C^2+S^2}} & C < 0,\ S = 0 \\ \cos\left(-\frac{\pi}{2}\right) = 0 = \frac{C}{\sqrt{C^2+S^2}} & C = 0,\ S < 0 \\ \text{undefined} & C = S = 0 \ . \end{cases}$$

Finally, we also write out κ^{e} to obtain

$$\begin{aligned} \kappa^{\mathrm{e}} \cos(\hat{x}^{\mathrm{e}}) &= \sqrt{C^2 + S^2}\, \frac{C}{\sqrt{C^2 + S^2}} \\ &= C = \kappa^{\mathrm{p}} \cos(\hat{x}^{\mathrm{p}}) + \kappa^{\boldsymbol{v}} \cos(\hat{z}) \ , \end{aligned}$$

which proves (14) and thus also (13) and (7).

Acknowledgment

This work is supported by the German Research Foundation (DFG) under grant HA 3789/16-1.

References

[1] M. Azmani, S. Reboul, J.-B. Choquel, and M. Benjelloun, "A Recursive Fusion Filter for Angular Data", in *IEEE International Conference on Robotics and Biomimetics (ROBIO 2009)*, 2009.

[2] M. S. Arulampalam, S. Maskell, N. Gordon, and T. Clapp, "A Tutorial on Particle Filters for Online Nonlinear/Non-Gaussian Bayesian Tracking", *IEEE Transactions on Signal Processing*, vol. 50, no. 2, pp. 174–188, 2002.

[3] F. Pfaff, G. Kurz, and U. D. Hanebeck, "Multimodal Circular Filtering Using Fourier Series", in *Proceedings of the 18th International Conference on Information Fusion (Fusion 2015)*, Washington D.C., USA, Jul. 2015.

[4] G. Kurz, F. Pfaff, and U. D. Hanebeck, "Application of Discrete Recursive Bayesian Estimation on Intervals and the Unit Circle to Filtering on SE(2)", *IEEE Transactions on Industrial Informatics*, vol. 14, no. 3, pp. 1197–1206, Mar. 2018.

[5] J. T. Kent, I. Hussein, and M. K. Jah, "Directional Distributions in Tracking of Space Debris", in *Proceedings of the 19th International Conference on Information Fusion (Fusion 2016)*, Jul. 2016.

[6] F. Pfaff, G. Kurz, C. Pieper, G. Maier, B. Noack, H. Kruggel-Emden, R. Gruna, U. D. Hanebeck, S. Wirtz, V. Scherer, T. Längle, and J. Beyerer, "Improving Multitarget Tracking Using Orientation Estimates for Sorting Bulk Materials", in *Proceedings of the 2017 IEEE International Conference on Multisensor Fusion and Integration for Intelligent Systems (MFI 2017)*, Daegu, Republic of Korea, Nov. 2017.

[7] S. Blackman and R. Popoli, *Design and Analysis of Modern Tracking Systems*. 1999.

[8] R. P. S. Mahler, *Statistical Multisource-Multitarget Information Fusion*. Artech House, Inc., 2007.

[9] M. Liggins II, D. Hall, and J. Llinas, *Handbook of Multisensor Data Fusion: Theory and Practice*, 2nd ed. CRC Press, 2009.

[10] O. E. Drummond, "Integration of Features and Attributes into Target Tracking", in *AeroSense 2000*, International Society for Optics and Photonics, 2000.

[11] ——, "Feature-, Attribute-, and Classification-Aided Target Tracking", in *International Symposium on Optical Science and Technology*, International Society for Optics and Photonics, 2001.

[12] G. Kurz, I. Gilitschenski, and U. D. Hanebeck, "Recursive Bayesian Filtering in Circular State Spaces", *IEEE Aerospace and Electronic Systems Magazine*, vol. 31, no. 3, pp. 70–87, Mar. 2016.

[13] F. Pfaff, "Multitarget Tracking Using Orientation Estimation for Optical Belt Sorting", Ph.D. dissertation, Karlsruhe Institute of Technology, defended on Nov. 13, 2018.

[14] A. Zygmund, *Trigonometric Series*, 3rd ed. Cambridge University Press, 2003, vol. 1 and 2.

[15] R. Jonker and A. Volgenant, "A Shortest Augmenting Path Algorithm for Dense and Sparse Linear Assignment Problems", *Computing*, vol. 38, no. 4, pp. 325–340, 1987.

[16] T. Hempel, *Mathematische Grundlagen, trigonometrische Funktionen (in German)*, Available online. http://www.uni-magdeburg.de/exph/mathe_gl/trigonometrische_funktionen.pdf.

[17] H. Haber, *Physics 116A: Mathematical Methods in Physics I*, Available online. http://scipp.ucsc.edu/~haber/ph116A/arg_11.pdf. 2011.